AMERICAN SOCIETY FOR MICROBIOLOGY | Molecular and Cellular Biology

AMPK Phosphorylates Desnutrin/ATGL and Hormone-Sensitive Lipase To Regulate Lipolysis and Fatty Acid Oxidation within Adipose Tissue

Sun-Joong Kim,[a] Tianyi Tang,[b] Marcia Abbott,[a] Jose A. Viscarra,[a] Yuhui Wang,[a] Hei Sook Sul[a,b]

Department of Nutritional Sciences and Toxicology[a] and Endocrinology Program,[b] University of California, Berkeley, California, USA

The role of AMP-activated protein kinase (AMPK) in promoting fatty acid (FA) oxidation in various tissues, such as liver and muscle, has been well understood. However, the role of AMPK in lipolysis and FA metabolism in adipose tissue has been controversial. To investigate the role of AMPK in the regulation of adipose lipolysis *in vivo*, we generated mice with adipose-tissue-specific knockout of both the α1 and α2 catalytic subunits of AMPK (AMPK-ASKO mice) by using aP2-Cre and adiponectin-Cre. Both models of AMPK-ASKO ablation show no changes in desnutrin/ATGL levels but have defective phosphorylation of desnutrin/ATGL at S406 to decrease its triacylglycerol (TAG) hydrolase activity, lowering basal lipolysis in adipose tissue. These mice also show defective phosphorylation of hormone-sensitive lipase (HSL) at S565, with higher phosphorylation at protein kinase A sites S563 and S660, increasing its hydrolase activity and isoproterenol-stimulated lipolysis. With higher overall adipose lipolysis, both models of AMPK-ASKO mice are lean, having smaller adipocytes with lower TAG and higher intracellular free-FA levels. Moreover, FAs from higher lipolysis activate peroxisome proliferator-activated receptor delta to induce FA oxidative genes and increase FA oxidation and energy expenditure. Overall, for the first time, we provide *in vivo* evidence of the role of AMPK in the phosphorylation and regulation of desnutrin/ATGL and HSL and thus adipose lipolysis.

Adipose tissue plays a key role in whole-body energy homeostasis by storing triacylglycerol (TAG) during excess energy intake, which is hydrolyzed (so-called lipolysis) to release fatty acids (FAs) into the circulation for use by other tissues during energy shortage. Thus, adipose TAG metabolism, especially the unique function of adipose lipolysis for FA release, must be exquisitely regulated according to nutritional conditions. For example, during fasting, lipolysis is stimulated upon the release of catecholamines to activate the β-adrenergic receptor-adenylyl cyclase-cyclic AMP (cAMP)-protein kinase A (PKA) pathway in adipocytes. In contrast, in the fed state, insulin released from pancreatic islet β cells activates phosphodiesterase 3B for degradation of cAMP in adipocytes, resulting in suppression of lipolysis (1). In addition to hormonal regulation, adipose lipolysis may also be regulated by the intracellular energy state for the maintenance of cellular TAG homeostasis.

AMP-activated protein kinase (AMPK) is a widely expressed multisubstrate serine/threonine kinase and a well-known sensor of the intracellular energy state that responds to metabolic stresses and other regulatory signals. AMPK is a heterotrimeric complex with a catalytic α subunit and two regulatory subunits, β and γ (2). There are several isoforms of each of the AMPK subunits, including two isoforms of the catalytic subunit, α1 and α2. AMPK is known to be activated allosterically by AMP but also is activated by phosphorylation of its catalytic subunit at T172 by the upstream kinases liver kinase B1 and calcium/calmodulin-dependent protein kinase kinase β (3). By sensing the cellular energy state, AMPK activation induces processes that produce ATP, such as FA oxidation, while inhibiting ATP-consuming synthetic pathways such as lipogenesis and gluconeogenesis (4–6). For example, AMPK-mediated phosphorylation and inactivation of acetyl coenzyme A (acetyl-CoA) carboxylase (ACC) reduces the malonyl-CoA concentration, relieving inhibition of carnitine palmitoyltransferase 1 (CPT1) to allow mitochondrial FA transport and oxidation in various tissues, such as muscle (4, 5). AMPK was reported also to phosphorylate transcription factors for lipogenesis, such as SREBP-1c, thereby decreasing lipogenic gene expression and lipogenesis in the liver (7). However, regulation of adipose tissue fat metabolism and lipolysis by AMPK is not clear.

TAG hydrolysis in adipose tissue occurs in a sequential manner from TAG, diacylglycerol (DAG), and monoacylglycerol (MAG) to produce three FAs and glycerol. We and others have identified desnutrin/ATGL (also called patatin-like phospholipase domain-containing protein 2) as the TAG hydrolase highly expressed in adipose tissue. Desnutrin/ATGL has been well accepted to execute the first step in TAG hydrolysis by converting TAG to DAG (8–12). Adipose-tissue-specific desnutrin/ATGL-overexpressing mice are leaner, with a smaller adipocyte size and decreased adipose-tissue TAG content (13). Conversely, both global knockout (KO) and adipose-tissue-specific KO of desnutrin/ATGL in mice result in an increased fat pad mass with severely reduced lipolysis (14, 15). Although classically thought to be a TAG hydrolase, hormone-sensitive lipase (HSL) is now considered a DAG hydrolase physiologically. Nevertheless, *in vitro*, HSL exhibits a broad substrate specificity and can catalyze the hydrolysis of TAG, DAG, and MAG, as well as cholesteryl and retinyl esters (16). However, the

Received 25 April 2016 **Returned for modification** 3 May 2016
Accepted 6 May 2016
Accepted manuscript posted online 16 May 2016
Citation Kim S-J, Tang T, Abbott M, Viscarra JA, Wang Y, Sul HS. 2016. AMPK phosphorylates desnutrin/ATGL and hormone-sensitive lipase to regulate lipolysis and fatty acid oxidation within adipose tissue. Mol Cell Biol 36:1961–1976. doi:10.1128/MCB.00244-16.

Address correspondence to Hei Sook Sul, hsul@berkeley.edu.

S.-J.K. and T.T. contributed equally to this work.

relative maximal rate of DAG hydrolysis has been shown to be much higher than for other substrates (17). In this regard, HSL-deficient (KO) mice are not obese but accumulate DAG in adipose tissue, further supporting the concept that HSL functions mainly as a DAG hydrolase (18, 19).

Lipolysis in adipose tissue is regulated by complex regulatory mechanisms themselves involving lipase, as well as lipid droplet-associated proteins. The first two steps in TAG hydrolysis, catalyzed by desnutrin/ATGL and HSL, are considered to be the regulatory steps in lipolysis. It has been well established that PKA-mediated phosphorylation of HSL and its translocation to the lipid droplets are critical for stimulated lipolysis (20, 21). Further, AMPK has been shown to phosphorylate HSL at S565 to prevent PKA-mediated phosphorylation at S563 and S660, significantly reducing epinephrine-stimulated lipolysis in cultured cells (22–25). Others, however, have reported that AMPK activation after epinephrine stimulation did not inhibit HSL activity (26). Making the issue more complicated, PKA has been reported to either activate or inhibit AMPK activity itself (27–29). As for desnutrin/ATGL, earlier studies suggested that PKA could not phosphorylate desnutrin/ATGL (11). Instead, we have shown that AMPK phosphorylates desnutrin/ATGL at S406 to increase its TAG hydrolase activity and thus lipolysis (15). However, others have reported that PKA phosphorylates S406 of desnutrin/ATGL for its activation. The role of AMPK in lipolysis is controversial at best.

While both catalytic subunits of AMPK, α1 and α2, are found in adipose tissue, global ablation of both α1 and α2 is lethal to mice. In order to investigate the role of AMPK in lipolysis and FA metabolism in adipose tissue under physiological conditions, we generated mice with adipose-tissue-specific KO of both the α1 and α2 subunits (AMPK-ASKO mice) by using aP2-Cre, as well as adiponectin (Adn)-Cre. Both of these AMPK-ASKO mice have defective phosphorylation of desnutrin/ATGL at S406, lowering its TAG hydrolase activity. In addition, these mice also have defective HSL phosphorylation at S565 that increases the phosphorylation of PKA sites, thus having enhanced catecholamine-stimulated lipolysis. Overall, with greater adipose lipolysis, AMPK-ASKO mice are lean, with greater energy expenditure, which is associated with higher adipose FA oxidation levels, as lipolytic products activate peroxisome proliferator-activated receptor delta (PPARδ).

MATERIALS AND METHODS

Animals. AMPKα1/α2 aP2-ASKO and Adn-ASKO mice were generated by first mating AMPKα1- and AMPKα2-floxed mice (kindly provided by the S. Morrison lab) to produce AMPKα1/α2-floxed mice, which were then mated with aP2-Cre^{Salk} and Adn-Cre mice. AMPKα1- and α2-floxed mice (30) contained the loxP sites flanking the third exon of the gene for α1 and the second exon of the gene for α2, which code for the respective kinase regions. Homozygous AMPKα1/α2 double-floxed mice were crossed with transgenic mice expressing Cre (aP2-Cre^{Salk}) (Jackson Laboratory) (31) or Adn-Cre (Jackson Laboratory) to generate adipose-tissue-specific AMPKα1/α2 double-KO mice, aP2-ASKO mice, and Adn-ASKO mice, respectively (Fig. 1B, top). We compared AMPKα1/α2 ASKO mice with AMPKα1/α2-floxed littermates on a C57BL/6J background. We provided either a standard chow diet (Harlan Teklad LM-485) or a high-fat diet (HFD; 45% of calories from fat, 35% of calories from carbohydrates, and 20% of calories from protein; Research Diets) *ad libitum* after weaning. The light was turned on at 7 a.m. and off at 7 p.m. Unless specified otherwise, mice were fasted and sacrificed at 9 a.m. for all experiments (10 p.m. for the lipolysis studies). All protocols were approved by the University of California at Berkeley Animal Care and Use Committee.

RT-qPCR. Total RNA was extracted with TRIzol reagent (Invitrogen), and cDNA was synthesized from 1 μg of total RNA by Superscript II reverse transcriptase (Invitrogen). Reverse transcription-quantitative PCR (RT-qPCR) with gene-specific primer sets was performed with an ABI7900 (Applied Biosystems). Gene expression levels were calculated by normalization to glyceraldehyde 3-phosphate dehydrogenase (GAPDH) by the $\Delta\Delta C_T$ method. The mean cycle threshold (C_T) was converted to a relative expression value by the $2^{-\Delta\Delta CT}$ method, and the range was calculated by the $2^{-(\Delta\Delta CT\ +\ \text{standard deviation of}\ \Delta\Delta CT)}$ method.

Immunoblotting. Total lysates were subjected to 8% SDS-PAGE, transferred to nitrocellulose, and probed with rabbit anti-desnutrin/ATGL (Cell Signaling), anti-phospho-desnutrin/ATGL S406 (Abcam), anti-GAPDH (Cell Signaling), anti-HSL (Cell Signaling), anti-phospho-HSL S563 (Cell Signaling), anti-phospho-HSL S565 (Cell Signaling), anti-phospho-HSL S660 (Cell Signaling), anti-ACC (Cell Signaling), anti-phospho-ACC S79, anti-AMPKα, anti-phospho-AMPKα (Cell Signaling), anti-AMPKα1, and anti-AMPKα2 (Santa Cruz) antibodies, followed by a horseradish peroxidase-conjugated secondary antibody (Bio-Rad). Blots were visualized by enhanced chemiluminescence (PerkinElmer), and images were captured with a Kodak Image Station 4000MM.

Immunoprecipitation. Lysates from white adipose tissue (WAT) in buffer containing 1% Triton X-100, 150 mM NaCl, 10% glycerol, 25 mM Tris [pH 7.4], phosphatase inhibitor cocktail (Cell Signaling), and protease inhibitor cocktail (Sigma) were incubated with antibodies against perilipin (Cell Signaling) at 4°C overnight, followed by the addition of 40 μl of protein A/G-agarose beads (Santa Cruz) and incubation for 1 h. Beads were collected by pulse centrifugation and washed five times with lysis buffer and heated to 99°C for 5 min in 5× SDS sample buffer. The input and the immunoprecipitated fraction were subjected to SDS-PAGE. HSL, perilipin, and GAPDH were detected by immunoblotting with each antibody.

Lipase activity measurements. For *in vitro* total lipase or TAG and DAG lipase activity measurements, lysates from WAT were prepared in radioimmunoprecipitation assay buffer supplemented with phosphatase inhibitor and protease inhibitor cocktails. For time-dependent lipase activity measurement, a fluorescent lipase assay (MarkerGene) was used. Briefly, tissues were homogenized in buffer A (50 mM Tris [pH 7.4], 0.1 M sucrose, 1 mM EDTA). An aliquot of 100 μg of the protein-rich infranatant was incubated with 50 μl of substrate reagent containing the fluorescent triglyceride 1,2-dioleoyl-3-(pyren-1-yl) decanoyl-rac-glycerol for the time indicated. The fluorescent FA released was measured with a microplate reader at 390 nm at each time point. TAG and DAG lipase activities were measured by the method of Schweiger et al. (32) with substrates containing 1.67 mM unlabeled triolein (Sigma) and 10 μCi/ml [carboxyl-^{14}C]triolein (American Radiolabeled Chemicals) or 0.3 mM unlabeled diolein (Sigma) and 10 μCi/ml 1-^{14}C-labeled diolein (1,3-dioleoylglycerol [1-^{14}C]oleoyl) (American Radiolabeled Chemicals). One hundred micrograms of the protein-rich infranatant was incubated with substrates at 37°C for 1 h. The reaction was terminated by the addition of 3.5 ml of methanol-chloroform-heptane (10:9:7). FAs were extracted with 1 ml of 0.1 M potassium carbonate–0.1 M boric acid (pH 10.5). The radioactivity of the upper phase was quantified by scintillation counting.

Lipolysis assay. Gonadal fat pads from mice were cut into 20-mg samples and incubated at 37°C without shaking in 500 μl of Krebs Ringer buffer (KRB; 12 mM HEPES, 121 mM NaCl, 4.9 mM KCl, 1.2 mM $MgSO_4$, 0.33 mM $CaCl_2$) containing 2% FA-free bovine serum albumin (BSA) and 0.1% glucose in the presence or absence of 10 μM isoproterenol (Sigma), 2 mM A-769662 (Sigma), 50 μM compound C/dorsomorphin (Sigma), 50 μM desnutrin/ATGL inhibitor atglistatin (Sigma), and 10 μM HSL inhibitor CAY10499 (Cayman). Lipolysis was assayed from the release of free FAs (FFAs) into the medium as described previously (15) with the NEFA C kit (Wako) and glycerol reagent (Sigma).

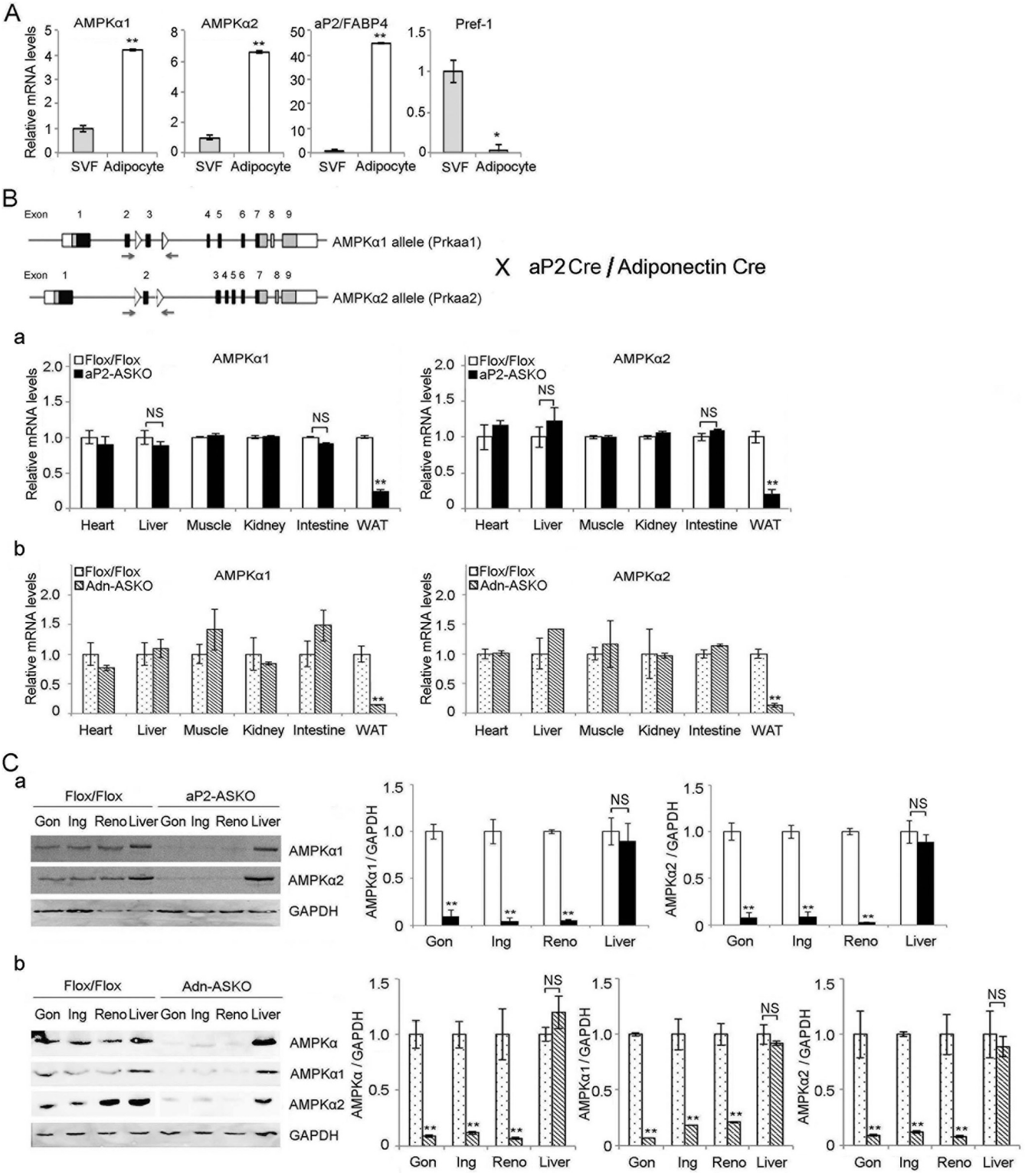

FIG 1 Generation of aP2 and Adn-AMPKα1/α2 ASKO mice. (A) RT-qPCR for AMPKα1 and AMPKα2 expression in the SVFs and adipocytes of wild-type mouse WAT ($n = 4$). (B) Cre-Lox strategy for removal of AMPKα1 (Prkaa1) and -α2 (Prkaa2) from adipose tissue. Open boxes, untranslated regions; gray boxes, translated regions that do not encode the kinase domain; black boxes, translated regions that encode the respective kinase domain; triangles, loxP sites; arrows, primer sets for genotyping (top). RT-qPCR for AMPKα1 (left) and AMPKα2 (right) expression in various tissues from aP2-ASKO (a) and Adn-ASKO (b) mice and control Flox/Flox mice ($n = 4$). (C) Immunoblotting and its quantification of lysates from various adipose depots, gonadal (Gon), inguinal (Ing), renal (Reno), and liver, from aP2-ASKO (a) and Adn-ASKO (b) mice with AMPKα, AMPKα1, and AMPKα2 antibodies. GAPDH was used as an internal control ($n = 4$). Data are expressed as means ± SEM. *, $P < 0.05$; **, $P < 0.01$; NS, no significant change. Experiments were repeated twice, and representative data are shown.

Adipocyte isolation. Gonadal fat pads were digested at 37°C for 1 h with collagenase (Roche) in KRB supplemented with 3 mM glucose and 1% FA-free BSA. Digestion products were filtered through nylon mesh and centrifuged. Adipocytes were collected from the upper phase.

Plasma metabolite measurements. Blood was centrifuged at 4°C for 15 min for fractionation. Triglyceride levels were measured with the Infinity triglyceride reagent (Thermo-Fisher), and nonesterified FAs (NEFAs) were measured with the NEFA C kit (Wako).

FA oxidation. FA oxidation in isolated adipocytes was determined by measuring $^{14}CO_2$ production and acid-soluble metabolites (ASMs) from [U-^{14}C]palmitic acid (0.2 μCi/ml) after incubation at 37°C for 1 h with gentle shaking. After acidification by the addition of 0.25 ml of 1 M perchloric acid, the mixture was maintained sealed at 37°C for an additional 60 min. Labeled CO_2 was trapped in 10 M KOH. Radioactivity trapped by KOH and that of ASMs were determined by liquid scintillation counting.

Lipogenesis assay. The lipogenesis assay was determined by quantifying the incorporation of D-[6-^{14}C]glucose (American Radiolabeled Chemicals) into lipids. Epididymal fat pads were washed twice with phosphate-buffered saline and incubated in KRB supplemented with 2% FFA BSA in the absence (basal) or presence of 1 μg/ml insulin (maximum lipogenesis response) for 15 min. D-Glucose (final concentration, 10 mM) containing 0.5 μCi/ml D-[^{14}C]glucose was added for 2 h. Subsequently, lipids were extracted from tissue explants as described by Folch et al. (33), with some modifications. Explants were transferred to extraction vials containing 2 ml of a 1:2 methanol-chloroform mixture and incubated for 1 h at room temperature, and 1 ml of 1% NaCl was added. After 16 h of incubation, the lower phase was collected. Extracted lipids were separated by thin-layer chromatography (TLC). After 10 min of iodine staining, TAG was scraped off and dissolved in toluene-polyphenol oxidase (Sigma) and radioactivity was quantified by scintillation counting.

ATP and AMP measurements. Cellular ATP and AMP levels were measured with the BioVision colorimetric/fluorometric assay and the Promega AMP-Glo kit, respectively, in accordance with the manufacturer's protocols.

PPAR binding activity. PPARδ and PPARα binding activities were measured with the PPARα, -δ, and -γ complete transcription factor assay kit (Cayman) by using nuclear extracts from WAT. Nuclear extracts were added to a plate coated with PPAR response element. After washing, antibodies specific to either PPARδ or PPARα were added. The reading of absorbance at 450 nm in a colorimetric plate reader was normalized to the positive-control value for each antibody for measurements of antibody efficiency and protein concentrations. To determine the effect of the PPARδ antagonist, AMPK-ASKO mice were injected intraperitoneally with GSK3787 (Sigma; 1 mg/kg/day) for 3 days. For the lipase inhibitor study, WAT explant samples were incubated with each lipase inhibitor before PPARδ binding activity measurement.

Adipocyte size determination. Gonadal fat samples were fixed in 10% buffered formalin, embedded in paraffin, cut into 8-μm-thick sections, and stained with hematoxylin and eosin. Adipocyte size was determined with NIH ImageJ software by measuring a minimum of 300 cells per slide, five slides per sample, and three or four mice per group.

Body composition. An EchoMRI-700 quantitative nuclear magnetic resonance analyzer (Echo Medical Systems) was used to measure the total fat and lean mass of mice.

Indirect calorimetry. Oxygen consumption (VO_2) and carbon dioxide production (VCO_2) were measured with a computer-controlled, open-circuit system (Oxymax Comprehensive Lab Animal Monitoring System; Columbus Instruments International). Data were normalized to body weight (BW) or lean body mass.

Statistical analysis. The results are expressed as means ± the standard errors of the means (SEM). Student's *t* test was used for comparisons of two groups. Unless specifically stated otherwise, all significance levels were set at $P < 0.05$. All experiments were repeated at least twice, and representative data are shown.

RESULTS

Generation of adipose-tissue-specific AMPKα1 and -α2 double-KO mice. To examine the role of AMPK in the regulation of desnutrin/ATGL and HSL in lipolysis within adipocytes, we first compared the expression levels of two isoforms of the AMPK catalytic subunit, α1 and α2, in the adipocyte fraction and the stromal vascular fraction (SVF), which contains various cell types, including preadipocytes, from adipose tissue of C57BL/6 wild-type mice. As expected, RT-qPCR showed that the expression level of aP2/FABP4 was markedly higher in the adipocyte fraction than in the SVF, whereas Pref-1 was expressed mainly in the SVF. More importantly, both AMPKα1 and -α2 subunits were detectable at a very low level in the SVF but the levels were approximately 5-fold higher in the adipocyte fraction than in the SVF (Fig. 1A).

Using the Cre-Lox strategy, we generated adipose-tissue-specific KO mice for both AMPKα1 and -α2 (AMPK-ASKO mice) by crossing mice carrying the conditional AMPK allele with two different Cre mouse lines, aP2-Cre and Adn-Cre, to generate aP2-ASKO and Adn-ASKO mice, respectively (Fig. 1B, top). Although aP2-Cre has been shown to be primarily expressed in adipocytes, it can also be found in macrophages and some blood lineage cells (31, 34). Therefore, we also used Adn-Cre, which is known to be more adipocyte specific. In comparison to that in control Flox/Flox mice, AMPKα1 expression in adipose tissue was lower by 80 and 90%, and AMPKα2 expression was lower by 80 and 92% in aP2-ASKO and Adn-ASKO mice, respectively (Fig. 1Ba and b). the AMPKα1 and -α2 protein levels in the WAT of aP2-ASKO mice were decreased by approximately 82 and 80%, respectively. In WAT of Adn-ASKO mice, the AMPKα1 and -α2 proteins were barely detectable, their levels being lower by approximately 94 and 90%, respectively (Fig. 1Cb). The lower AMPKα1 and -α2 protein levels were detected in all of the fat depots examined, such as the gonadal, inguinal, and renal depots of aP2-ASKO and Adn-ASKO mice (Fig. 1C). In contrast, AMPKα1 and AMPKα2 expression remained similar in all of the other tissues examined, including heart, liver, muscle, kidney, and intestine tissues (Fig. 1Ba and b). These results demonstrate that the AMPKα1 and -α2 levels were greatly reduced specifically in the adipose tissue of both aP2-ASKO and Adn-ASKO mice.

AMPK phosphorylates desnutrin/ATGL and HSL in adipose tissue. We previously reported that desnutrin/ATGL can be phosphorylated at serine-406 (S406) by AMPK to increase its catalytic activity and thus lipolysis (15). Therefore, we examined desnutrin/ATGL phosphorylation in aP2-ASKO and Adn-ASKO mice. Immunoblotting and quantification of WAT lysates showed that although total desnutrin/ATGL levels were not changed in AMPK-ASKO mice, phosphorylation of desnutrin/ATGL at S406 was markedly lower, at almost undetectable levels, in WAT of both aP2-ASKO and Adn-ASKO mice than in that of control Flox/Flox mice (Fig. 2A). These *in vivo* results are in agreement with our previous report that S406 of desnutrin/ATGL is phosphorylated by AMPK. We next examined HSL, which is phosphorylated by PKA at S563 and S660 to increase HSL translocation to lipid droplets and activate its lipolytic activity. HSL is known to be phosphorylated also by AMPK at S565 to prevent PKA phosphorylation at S563, and possibly S660, to inhibit HSL activity in cultured cells (22, 35). Immunoblotting with antibodies against site-specific phosphorylation of HSL showed that phosphorylation of HSL at S565 was markedly lower and barely detectable in both

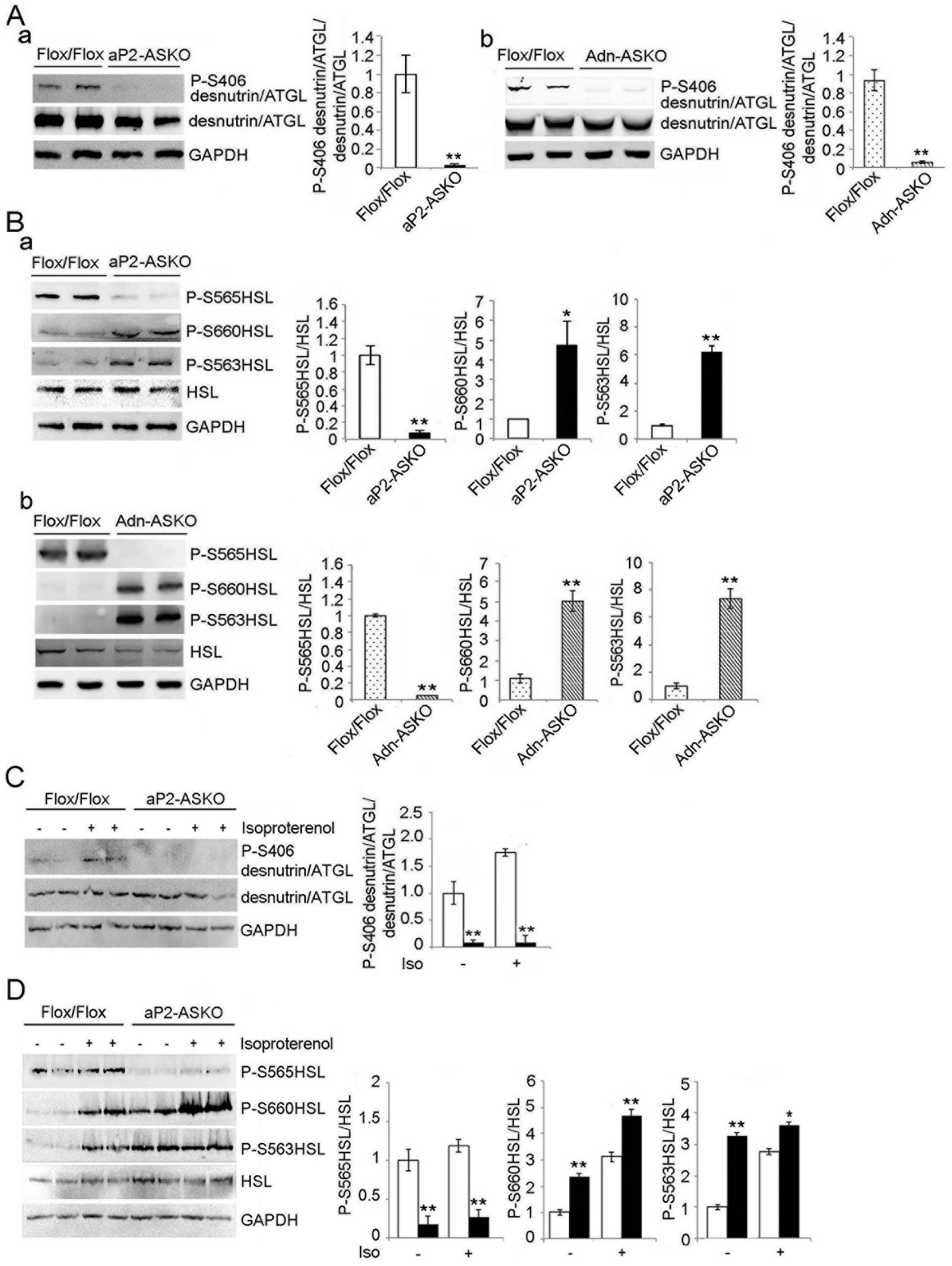

FIG 2 AMPK phosphorylates desnutrin/ATGL and HSL. (A) Immunoblotting and its quantification of WAT lysates with antibodies against phosphorylated desnutrin/ATGL (P-S406) and total desnutrin/ATGL in aP2-ASKO (a) and Adn-ASKO (b) mice. WAT were harvested under fasted conditions (9 a.m.). (B) Immunoblotting and its quantification of WAT lysates with antibodies against HSL and phospho-HSL (P-S565, P-S660, and P-S563) in aP2-ASKO (a) and Adn-ASKO (b) mice ($n = 4$). (C and D) Immunoblotting and its quantification of desnutrin/ATGL and its phosphorylation (C) and HSL and its phosphorylation (D) in WAT lysates under basal or isoproterenol (Iso)-stimulated conditions ($n = 4$). Experiments were repeated twice, and a representative blot is shown. *, $P < 0.05$; **, $P < 0.01$.

aP2-ASKO and Adn-ASKO mouse WAT than in Flox/Flox mice, whereas phosphorylation at PKA sites S563 and S660 was higher (Fig. 2B). These results demonstrate for the first time *in vivo* that S565 of HSL is phosphorylated by AMPK and that lack of S565 phosphorylation increases PKA phosphorylation of HSL.

We next cultured WAT explants in the presence of a β-adrenergic agonist, isoproterenol, to examine potential cross talk between AMPK and PKA. As predicted, immunoblotting of desnutrin/ATGL phosphorylation at S406 in WAT from aP2-ASKO was not clearly detectable under basal or isoproterenol-stimulated conditions. In contrast, Flox/Flox mice showed low but clearly detectable desnutrin/ATGL phosphorylation at S406 under basal conditions, which was further increased upon isoproterenol treatment (Fig. 2C). These results are consistent with the report that PKA can cross talk and activate AMPK (28, 36). We also examined HSL phosphorylation upon isoproterenol treatment. As predicted, HSL phosphorylation at PKA sites S563 and S660 in WAT of Flox/Flox mice was greatly increased upon isoproterenol treatment. Phosphorylation of the AMPK site at S565 was increased about 20%, although not statistically significantly so, upon isoproterenol treatment. In WAT of aP2-ASKO mice, S565 phosphorylation of HSL was barely detectable under basal conditions and remained the same after isoproterenol treatment, whereas S563 and S660 phosphorylation was considerably higher in WAT of aP2-ASKO mice than in that of Flox/Flox mice under basal conditions and was increased further upon isoproterenol treatment (Fig. 2D). Overall, these results are consistent with the report that PKA can cross talk and activate AMPK to phosphorylate the lipases desnutrin/ATGL and HSL in adipose tissue. More importantly, these results again show that AMPK phosphorylates S406 of desnutrin/ATGL, as well as S565 of HSL, which diminishes PKA phosphorylation at S563 and S660 of HSL.

Regulation of desnutrin/ATGL and HSL activity by AMPK. We next examined the effect of AMPK deficiency on lipase activity *in vitro* by using WAT lysates from Flox/Flox and ASKO mice. First, we measured lipase activity via a fluorescent-lipase assay method. We detected lipase activity in Flox/Flox samples, which was increased up to 40 min of incubation in a time-dependent manner. More importantly, the lipase activity in WAT lysates from aP2-ASKO mice were higher than those in Flox/Flox mouse samples (Fig. 3Aa, left side). We also measured lipase activity by using the radiolabeled substrate [carboxyl-^{14}C]triolein, and FA extracted from the incubation mixture showed significantly higher (55% higher) levels in aP2-ASKO than Flox/Flox samples after a 60-min reaction (Fig. 3Aa, middle). The use of [1-^{14}C]dioleln (1,3-dioleoylglycerol [1-^{14}C]oleoyl) also showed higher lipase activity (Fig. 3Aa, right side). Similar result was obtained when Adn-ASKO mouse WAT was used in the lipase assay (Fig. 3Ab).

Since the lipase activity was from the combination of desnutrin/ATGL and HSL activity, to further investigate the effect of AMPK deficiency on each lipase, we used lipase-specific inhibitors in lipase activity assays. In the presence of the HSL inhibitor CAY10499, lipase activity was lower by approximately 20 and 24% in aP2-ASKO and Adn-ASKO mouse WAT, respectively, than that in Flox/Flox mouse WAT (Fig. 3B), reflecting the fact that desnutrin/ATGL activity was lower because of AMPK deficiency from lack of S406 phosphorylation. On the other hand, in the presence of the desnutrin/ATGL inhibitor atglistatin, the lipase activity was approximately 27% higher in aP2-ASKO than in Flox/Flox samples. A greater difference in lipase activity was detected when an Adn-ASKO sample was used (Fig. 3C). These results reflected the fact that the lack of AMPK-mediated phosphorylation of S565 prevented inhibition of HSL phosphorylation at S563 and S660.

Effects of AMPK ablation on basal and stimulated lipolysis. We next examined the effects of AMPK deficiency on adipose lipolysis. Explants of WAT were harvested from mice under postprandial (basal) conditions and incubated in the absence or presence of isoproterenol (β-adrenergic agonist, PKA activator). Under basal conditions, the FFA release level was lower in both aP2-ASKO and Adn-ASKO mice than in Flox/Flox mice. This was particularly significant in the Adn-ASKO mice, probably because of more complete ablation than in aP2-ASKO mice (Fig. 4Aa and b). There was no difference between the AMP/ATP ratios of Adn-ASKO and Flox/Flox mouse WAT samples (Fig. 4Ac, left). However, as predicted, AMPK and T172-phosphorylated AMPK levels were much lower than in Flox/Flox mice (Fig. 4Ac, right), which correlated with less FFA release in Adn-ASKO mice, demonstrating the role of AMPK in basal lipolysis. In the presence of isoproterenol, FFA release was significantly higher in WAT explants from both aP2-ASKO and Adn-ASKO mice than in those from Flox/Flox mice (Fig. 4Aa and b). Upon lipolytic stimulation, HSL is known to be translocated from the cytoplasm to the lipid droplet to interact with perilipin, which is phosphorylated by PKA (17, 37, 38). Indeed, immunoprecipitation with perilipin antibody, followed by immunoblotting with HSL antibody, detected significantly greater binding of HSL to perilipin in WAT of AMPK-ASKO mice than in WAT of Flox/Flox mice (Fig. 4B). These results indicate that, in contrast to that under basal conditions, lipolysis was higher in AMPK-ASKO under stimulated conditions.

We also explored the effects of the AMPK activator A-769662 and the AMPK inhibitor compound C on WAT explants. Under basal conditions, FFA release was 33% higher upon A-769662 treatment but 10% lower upon compound C treatment in Flox/Flox mice. On the other hand, FFA release did not change upon treatment with either A-769662 or compound C in both aP2-ASKO and Adn-ASKO mice (Fig. 4C). We also used an additional AMPK activator, 5-aminoimidazole-4-carboxamide-1-β-D-ribofuranoside (AICAR), and obtained data similar to those obtained with A-769662 (data not shown). These results, overall, indicate that AMPK plays a positive role in basal lipolysis, reflecting AMPK phosphorylation/activation of desnutrin/ATGL and the lack of desnutrin/ATGL activation in AMPK deficiency. Under stimulated conditions, FFA release was 18% lower upon A-769662 treatment and 25% higher upon compound C treatment in Flox/Flox mice. Furthermore, in both aP2-ASKO and Adn-ASKO mice, FFA release did not change upon treatment with either A-769662 or compound C (Fig. 4C), demonstrating the inhibitory role of AMPK in lipolysis under stimulated conditions, reflecting the AMPK phosphorylation of HSL that prevents PKA phosphorylation/activation of HSL and lack of this inhibitory effect of AMPK on our AMPK-ASKO mice under stimulated conditions. To exclude the possible contribution of FFA release from macrophages and blood cell types (the aP2 promoter has been reported to be active in macrophages and some blood cell types as well), we next isolated adipocytes from WAT of aP2-ASKO mice to examine lipolysis. Indeed, we detected a greater difference in FFA release from adipocytes under basal conditions. FFA release was 40% higher upon A-769662 treatment and 70% lower upon compound

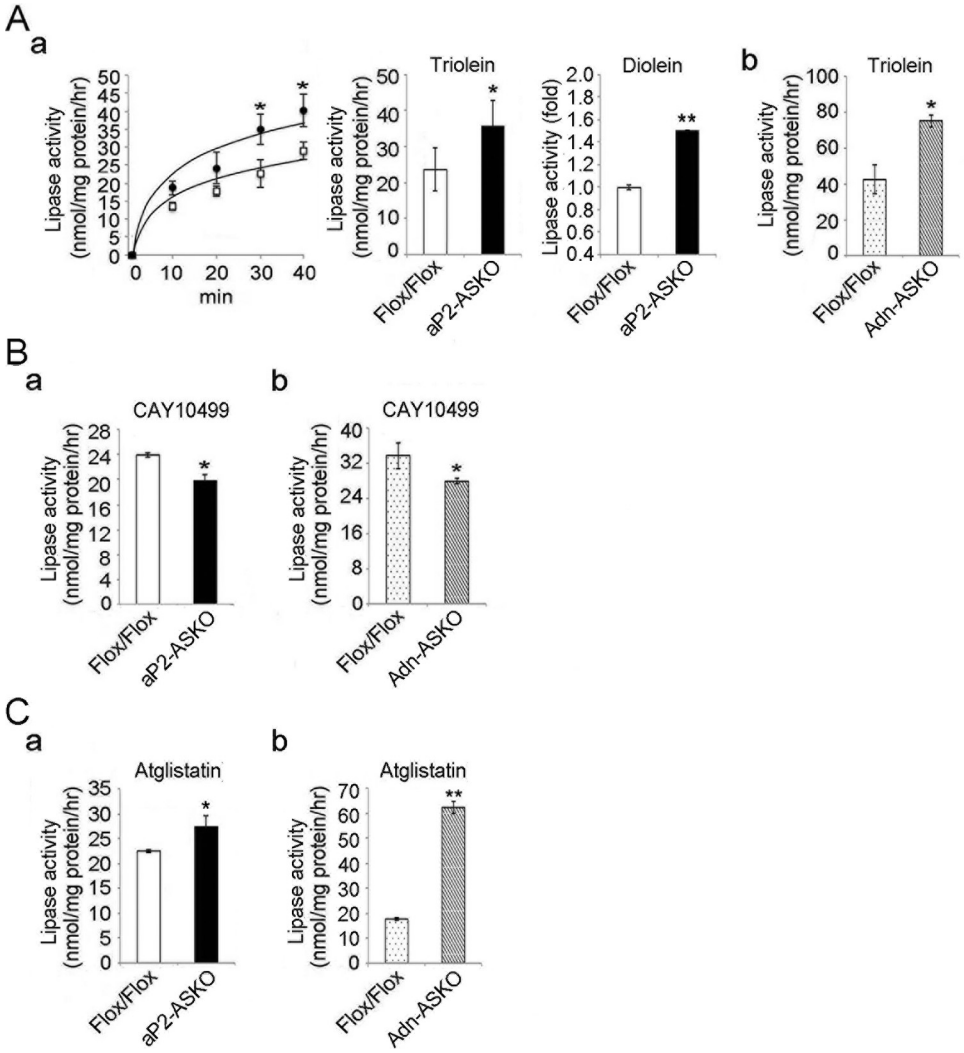

FIG 3 Effect of AMPK on lipase activities. (A) Fluorescent-lipase assay with pyrene-labeled TAG (1,3-dioleolyl-3-(pyren-1-yl) decanoyl-rac-glycerol) (a, left) and lipase activities with [carboxyl-^{14}C]triolein (a, middle) and [1-^{14}C]diolein (1,3-dioleoylglycerol [1-^{14}C]oleoyl) (a, left) as substrates for WAT lysates from aP2-ASKO mice (a) and lipase activity with [^{14}C]triolein as a substrate for WAT lysates from Adn-ASKO mice (b) ($n = 4$). (B) Lipase activities with a [^{14}C]triolein substrate in the presence of 10 μM HSL inhibitor CAY10499 in aP2-ASKO (a) or Adn-ASKO (b) mouse WAT. (C) Lipase activities with [^{14}C]triolein in the presence of the desnutrin/ATGL inhibitor atglistatin at 50 μM in aP2-ASKO (a) or Adn-ASKO (b) mouse WAT. Data are expressed as means ± SEM. *, $P < 0.05$; **, $P < 0.01$. Experiments were repeated twice, and representative data are shown.

C treatment in Flox/Flox mice, while no changes in FFA release were observed in aP2-ASKO adipocytes. These results demonstrate the stimulatory effect of AMPK on basal lipolysis in control WAT. Under stimulated conditions, FFA release was decreased by 47% upon A-769662 treatment and increased by 29% upon compound C treatment in control WAT. On the other hand, consistent with the results obtained in WAT explant experiments, FFA release in AMPK-deficient adipocytes did not change upon either AMPK activation or inhibition (Fig. 4D).

We also examined lipolysis in the presence of specific lipase inhibitors. Under basal conditions, FFA release was 16.5% lower after atglistatin treatment in control Flox/Flox samples but was unchanged when CAY10499 was used. Although the degree of inhibition by atglistatin was not marked, lack of inhibition by CAY10499 suggests that desnutrin/ATGL primarily regulates lipolysis under basal conditions. More importantly, in AMPK-ASKO samples, FFA release was lower than that in Flox/Flox samples and treatment with either atglistatin or CAY10499 did not affect lipolysis, further substantiating the role of desnutrin/ATGL under basal conditions (Fig. 4E, left). Under stimulated conditions, we detected a 20% decrease in FFA release in control Flox/Flox samples treated with either atglistatin or CAY10499, indicating the roles of both desnutrin/ATGL and HSL in stimulated lipolysis. More importantly, under stimulated conditions, FFA release showed no significant change upon atglistatin treatment but was 37% lower upon CAY10499 treatment in AMPK-ASKO samples (Fig. 4E, right), further confirming that the greater lipolysis in AMPK-ASKO mice was due to HSL activity under stimulated conditions.

Deficiency of AMPK in adipose tissue causes a lean phenotype. We examined the phenotypes of aP2-ASKO and Adn-ASKO mice. There is no difference between AMPK-ASKO and Flox/Flox

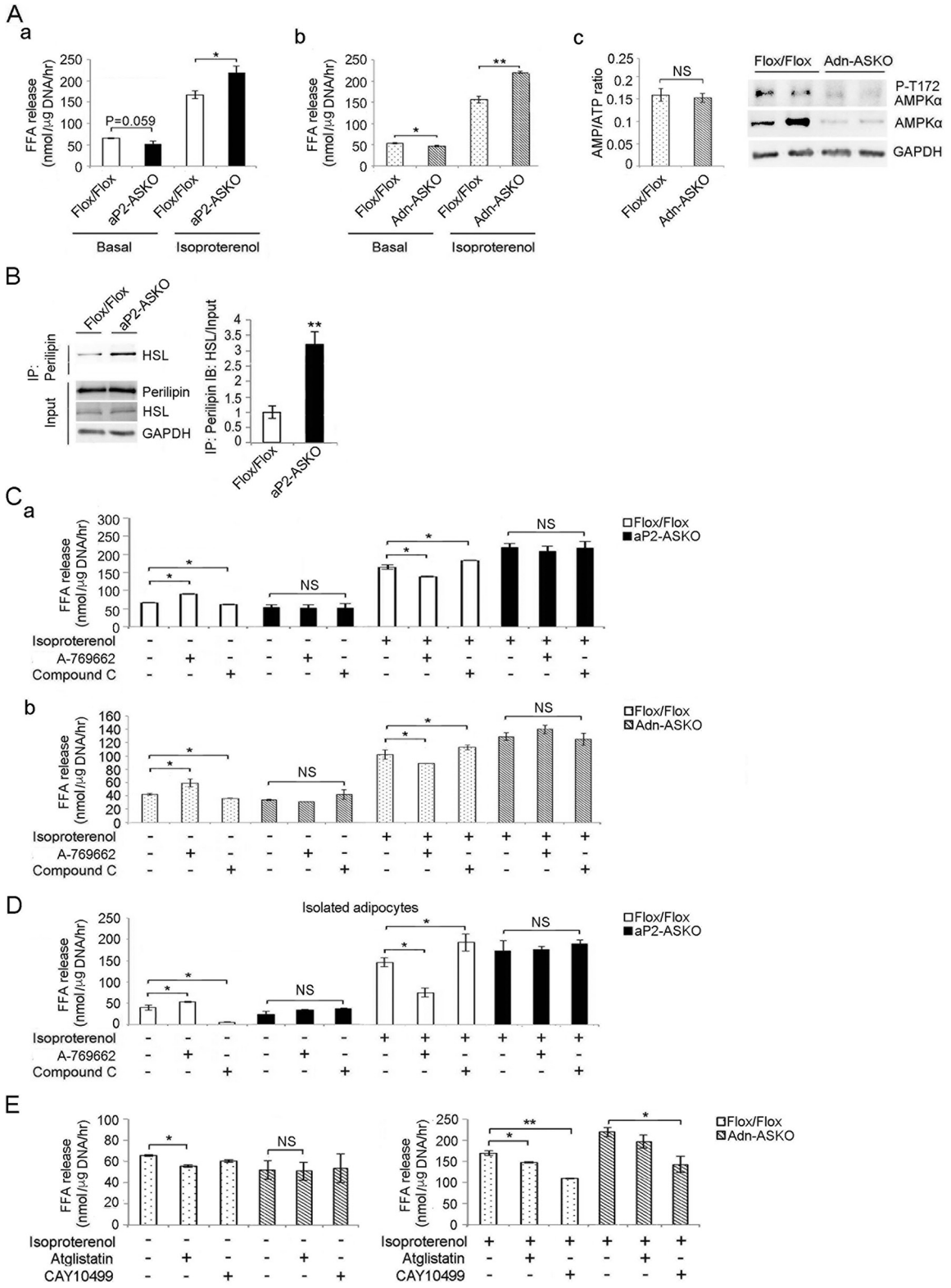

FIG 4 AMPK induces basal lipolysis and inhibits stimulated lipolysis. (A) FFA release from WAT of aP2-ASKO (a) and Adn-ASKO (b) mice under basal and isoproterenol-stimulated conditions. Cellular AMP/ATP ratios in WAT of Flox/Flox and Adn-ASKO mice under basal conditions (c, left) and immunoblotting for AMPKα and AMPKα phosphorylated at T172 (c, right). (B) Immunoblotting with HSL antibody after immunoprecipitation (IP) of WAT lysates with perilipin antibody. (C) FFA release from WAT of aP2-ASKO (a) and Adn-ASKO (b) mice upon treatment with 2 mM A-769662 or 50 μM compound C under basal or stimulated conditions ($n = 5$). (D) FFA release from isolated adipocytes of aP2-ASKO mice upon treatment with 2 mM A-769662 or 50 μM compound C under basal and stimulated conditions ($n = 4$). (E) FFA release from Adn-ASKO mouse WAT explants upon treatment with 50 μM atglistatin or 10 μM CAY10499 under basal and isoproterenol-stimulated conditions. Data are expressed as means ± SEM. *, $P < 0.05$; **, $P < 0.01$; NS, no significant change. Experiments were repeated twice, and representative data are shown.

littermates at weaning. Under a chow diet, BW started to be significantly lower in aP2-ASKO and Adn-ASKO mice than in Flox/Flox mice at 14 and 10 weeks of age, respectively. The difference was even more pronounced and lower by approximately 20% at 20 and 12 weeks, respectively (Fig. 5Aa and b, left two parts). No changes in food intake were observed among these mouse lines. Fat mass measured by EchoMRI was also lower by 34 and 36% in aP2-ASKO and Adn-ASKO mice, respectively, than in Flox/Flox mice. No change in lean body mass was observed (Fig. 5Aa and b, right two parts). Fat pads, including the gonadal, inguinal, and renal depots, weighed approximately 33, 28, and 44% less, respectively, in both aP2-ASKO and Adn-ASKO mice than in Flox/Flox mice. We did not find differences in brown adipose tissue (BAT) mass or liver weight between AMPK-ASKO and Flox/Flox mice (Fig. 5B). Similar differences were observed in mice on an HFD (data not shown).

Histological analysis of gonadal WAT showed smaller adipocytes in aP2-ASKO mouse WAT. Quantification of adipocyte size indicated a greater frequency of smaller adipocytes and a lower frequency of midsize or larger adipocytes in aP2-ASKO mice than in Flox/Flox mice (Fig. 5C). Adipose tissue TAG content per unit of DNA was lower by 10% and DAG content was lower by 90% in aP2-ASKO mouse WAT than in Flox/Flox mouse WAT (Fig. 5D, left and middle parts), whereas the liver TAG content was not different in AMPK-ASKO mice at 16 weeks (data not shown). In contrast, NEFA levels in WAT were 2.5-fold higher in aP2-ASKO mice (Fig. 5D, right part), whereas serum NEFA levels showed an approximately 50% increase in both aP2-ASKO and Adn-ASKO mice (Fig. 5E).

We also examined adipocyte differentiation markers in WAT and found no changes in the expression of these markers, such as C/EBPα, C/EBPβ, and PPARγ (data not shown), indicating that there was no effect on adipose differentiation. AMPK has been reported to regulate the transcription of lipogenic transcription factors (39, 40). We therefore examined the expression levels of lipogenic genes. Expression of lipogenic markers, including FA synthase, ACCα, mitochondrial glycerol-3-phosphate acyltransferase, and stearoyl-CoA desaturase 1, was significantly higher by 1.7-, 4.0-, 3.8-, and 6.0-fold, respectively, in aP2-ASKO mouse WAT than in Flox/Flox mouse WAT (Fig. 5Fa). ACC is phosphorylated by AMPK at S79 to inhibit its activity. We found that phosphorylation of ACC was markedly lower in ASKO mice than in Flox/Flox mice (Fig. 5Fb). We also measured TAG synthesis by incubating WAT explants with [^{14}C]glucose and found that TAG synthesis was higher under both non-insulin-treated and insulin-treated conditions in Adn-ASKO mouse WAT than in Flox/Flox mouse WAT (Fig. 5Fc). These results exclude the possibility that the lean phenotype of AMPK-ASKO mice was due to decreased lipogenesis. These results are consistent with previous reports of an inhibitory effect of AMPK on lipogenesis (41).

Increased lipolysis in AMPK deficiency promotes FA oxidation in WAT. We found that the total oxygen consumption rate was approximately 17% higher in aP2-ASKO mice than in Flox/Flox mice (Fig. 6A, left and middle). The respiratory exchange ratio (RER) was lower in AMPK-ASKO mice than in Flox/Flox mice (0.77 versus 0.83) (Fig. 6A, right), suggesting greater fat oxidation in ASKO mice. Similar results were obtained with mice on an HFD (data not shown). These results suggest that AMPK-ASKO mice have higher energy expenditure and fat utilization.

Next, we examined FA oxidation in WAT. FA oxidation was evaluated by measuring captured CO_2 levels and ASMs after incubation of WAT explants with [^{14}C]palmitate. Captured CO_2 and ASM levels were 48 and 34% higher, respectively, in aP2-ASKO mouse WAT than in Flox/Flox mouse WAT after 40 min of incubation. The difference was even greater after 60 min of incubation. Similar results were obtained with Adn-ASKO mice, showing captured CO_2 and ASM levels after 60 min of incubation to be 35 and 38% higher, respectively, in Adn-ASKO mouse WAT than in Flox/Flox mouse WAT (Fig. 6Ba and b). No changes in FA oxidation were observed in liver or muscle samples from AMPK-ASKO mice (Fig. 6Bc and d).

Furthermore, expression levels of FA oxidation-related genes, such as those for CPT1 and -2, hydroxyacyl-CoA dehydrogenase/3-ketoacyl-CoA thiolase/enoyl-CoA hydratase, acyl-CoA oxidase 1, palmitoyl CoA oxidase 1, malate dehydrogenase 2, cytochrome *c* oxidase subunit VIIIb (Cox8b), and very-long-chain acyl-CoA dehydrogenase, were significantly higher in aP2-ASKO and Adn-ASKO mouse WAT than in Flox/Flox mouse WAT (Fig. 6Ca and b). There was no difference in expression levels of these oxidative genes in the liver between AMPK-ASKO and Flox/Flox mice (Fig. 6Cc and d). These results indicate that AMPK deficiency results in increased FA oxidation, contributing to the lean phenotype of AMPK-ASKO mice.

Excessive lipolysis promotes FA oxidation through PPARδ. FA oxidative genes are known to be transcriptionally activated by PPARα or PPARδ (42), and lipolysis might provide ligands for PPARα or PPARδ. In WAT, the PPARα expression level was very low, whereas the PPARδ expression level was 5.8-fold higher than that of PPARα (Fig. 7Aa, left). There was no difference in the DNA binding activity of PPARα in WAT lysates between AMPK-ASKO and Flox/Flox mice. In contrast, PPARδ binding was 1.4- and 1.9-fold higher in aP2-ASKO and Adn-ASKO mice than in Flox/Flox mice, respectively (Fig. 7Aa, right, and b). Furthermore, administration of the PPARδ antagonist GSK3787 to aP2-ASKO and Adn-ASKO mice lowered the DNA binding activity of PPARδ, but not that of PPARα, to the level of wild-type mice (Fig. 7B). These results indicate the specificity of the effect of GSK3787 on PPARδ binding and the higher PPARδ binding activity in WAT of aP2-ASKO and Adn-ASKO mice. In addition, GSK3787 treatment effectively reduced the expression of FA oxidative genes in WAT of aP2-ASKO and Adn-ASKO mice (Fig. 7C), further indicating that PPARδ was involved in inducing FA oxidative genes and FA oxidation in AMPK-deficient mice.

We also examined PPARδ binding and Cox8b expression in WAT after treatment with lipase inhibitors. Treatment with the desnutrin/ATGL inhibitor atglistatin decreased PPARδ binding activity and Cox8b expression in WAT of Flox/Flox mice but not in that of Adn-ASKO mice. In contrast, treatment with the HSL inhibitor CAY10499 decreased PPARδ binding activity and Cox8b expression to a greater extent in Adn-ASKO mouse WAT than in Flox/Flox mouse WAT (Fig. 7D). These results further show that greater lipolysis from HSL activity in AMPK-ASKO mice produced ligands for PPARδ, resulting in induction of FA oxidative genes and promotion of FA oxidation.

DISCUSSION

AMPK is considered to be a key sensor of the energy state of cells and is activated upon energy depletion to enhance FA oxidation for ATP production. However, how AMPK regulates lipolysis within adipose tissue whose unique metabolic function is to re-

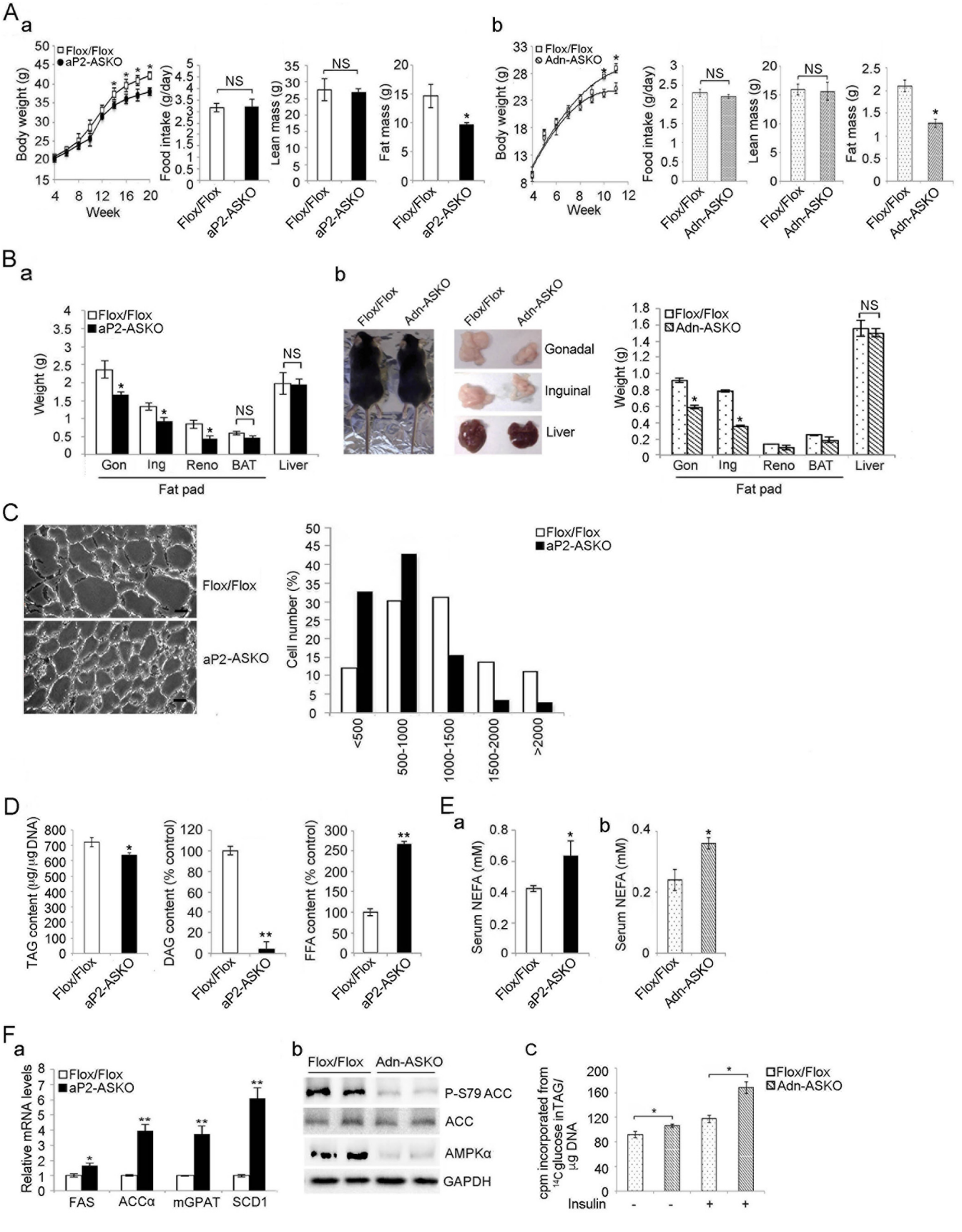
A
a
Flox/Flox
aP2-ASKO
Body weight (g)
Week
Food intake (g/day)
Lean mass (g)
Fat mass (g)
NS
b
Flox/Flox
Adn-ASKO
B
a
Weight (g)
Gon
Ing
Reno
BAT
Liver
Fat pad
b
Gonadal
Inguinal
Liver
C
Flox/Flox
aP2-ASKO
Cell number (%)
<500
500-1000
1000-1500
1500-2000
>2000
D
TAG content (μg/μg DNA)
DAG content (% control)
FFA content (% control)
E
a
Serum NEFA (mM)
b
F
a
Relative mRNA levels
FAS
ACCα
mGPAT
SCD1
b
P-S79 ACC
ACC
AMPKα
GAPDH
c
cpm incorporated from 14C glucose in TAG/μg DNA
Insulin

lease FAs into circulation during an organism's energy shortage is not clear. It has been reported that PKA activation by isoproterenol or forskolin treatment promotes the phosphorylation of AMPK at T172 to increase lipolysis in adipocytes in culture (36). Global AMPKα2 KO mice on an HFD had exacerbated adiposity (43), whereas chronic AICAR treatment of rodents reduced adiposity (44), suggesting enhancement of lipolysis by AMPK. In contrast, others have reported that activation of AMPK by AICAR strongly reduced isoproterenol-induced lipolysis, showing an antilipolytic effect of AMPK (22). Furthermore, phosphorylation of AMPK by PKA was reported to prevent T172 phosphorylation of AMPK to decrease its activity in adipocytes (29). On the other hand, others have reported that PKA increases AMPK phosphorylation at T172 and its activity in primary adipocytes (28). These conflicting effects of AMPK on adipocyte lipolysis and the inconsistent function of PKA in AMPK phosphorylation/activation reported to date underscore the need for a comprehensive *in vivo* study under physiological settings.

In our present study, we generated mouse models with both AMPKα1 and -α2 ablated in adipose tissue via the use of aP2-Cre and Adn-Cre to examine the role of AMPK specifically in adipose lipases and lipolysis. We found that AMPK ablation in adipose tissue diminishes desnutrin/ATGL phosphorylation and thus its activity, resulting in a lower basal lipolysis level. On the other hand, HSL activation under catecholamine-stimulated conditions was significantly higher, with an overall increase in lipolysis resulting in a lean phenotype. Here, we propose that AMPK has opposing effects on desnutrin/ATGL and HSL. We propose that, under basal conditions, AMPK activates lipolysis by phosphorylating desnutrin/ATGL to maintain an appropriate degree of lipolysis. However, AMPK phosphorylation of HSL under stimulated conditions inhibits PKA phosphorylation and activation, resulting in suppression of lipolysis, potentially for prevention of excessive FA-TAG recycling.

Desnutrin/ATGL catalyzes the first step in adipose lipolysis and is regarded as critical in the regulation of lipolysis. However, it has not been clear how desnutrin/ATGL is regulated by AMPK under physiological conditions *in vivo*. Previously, we reported that desnutrin/ATGL is activated by AMPK via phosphorylation on S406 (human S404) and mutation of this site decreases lipase activity (15, 45). In contrast, Watt and colleagues reported that the phosphorylation of this site was increased not by AMPK activation but by β-adrenergic stimulation, suggesting PKA-mediated phosphorylation at S406 (46) for stimulated lipolysis. In the present study, we found an increase in lipolysis when using the AMPK activator AICAR or A-769662 in both WAT explants and isolated adipocytes, whereas the AMPK inhibitor compound C decreased lipolysis. More importantly, ablation of both catalytic subunits α1 and α2 of AMPK in adipose tissue caused a decrease in the phosphorylation of desnutrin/ATGL on S406 and a reduction in TAG hydrolase activity, accompanying a decrease in lipolysis in WAT under basal conditions. These results demonstrate that the major role of desnutrin/ATGL is to break down TAG through AMPK-mediated phosphorylation of desnutrin/ATGL in the basal state of adipocytes. In addition to S406, desnutrin/ATGL has also been shown to be phosphorylated at S430 in mice (human S428), which is a PKA consensus site, but the function of this phosphorylation remains unknown (45). Moreover, in *Caenorhabditis elegans*, the desnutrin/ATGL orthologue ATGL-1 is phosphorylated at multiple sites (none of them matching S406) for its inactivation (47) and at one such phosphorylation site to affect protein stability. In addition, desnutrin/ATGL protein levels in mammals have been reported to increase upon AICAR treatment (48). As for the desnutrin/ATGL levels, we previously reported a drastic induction of desnutrin/ATGL expression by glucocorticoids (8). In our present study, we did not detect any changes in desnutrin/ATGL levels in AMPK-ASKO mice. Moreover, desnutrin/ATGL is known to interact with comparative gene identification 58 (CGI-58) to increase its TAG hydrolase activity (49). Desnutrin/ATGL interaction with CGI-58 requires phosphorylation of perilipin by PKA for dissociation of the perilipin–CGI-58 complex. Here, we propose that TAG lipase activity of desnutrin/ATGL under basal conditions probably is not from its interaction with CGI-58 but by its phosphorylation by AMPK. This is supported by a previous report showing that lipolysis is controlled mainly by desnutrin/ATGL under basal conditions (50). In this regard, Lodish and coworkers reported that, upon insulin treatment, FAs transported into adipocytes could be converted into fatty acyl-CoA for further metabolism, a step that utilizes ATP to generate AMP, allowing AMPK activation (51). In any case, our results clearly show decreased desnutrin/ATGL phosphorylation and its activity in AMPK deficiency, demonstrating the role of AMPK *in vivo* for desnutrin/ATGL activity and lipolysis under basal conditions.

In contrast to desnutrin/ATGL, HSL is a well-known classic target of PKA for lipolysis under stimulated conditions. Phosphorylation at S660 and S563 by PKA has been shown to increase HSL translocation to lipid droplets and its enzymatic activity (52). Furthermore, phosphorylation at S565 by AMPK was reported to decrease in HSL activity upon PKA stimulation in cultured cells (22, 53) by inhibiting S563 and S660 phosphorylation by PKA (22). However, others did not observe this decrease in HSL activity upon AICAR treatment (26). In our present study, unlike under basal conditions, treatment with the AMPK activator A-769662 decreased isoproterenol-stimulated lipolysis in wild-type WAT, whereas treatment with the AMPK inhibitor compound C increased it, suggesting the inhibitory role of AMPK phosphorylation in the PKA-mediated phosphorylation and activation of HSL. More importantly, S565 phosphorylation was markedly lower in

FIG 5 AMPK-ASKO mice show a lean phenotype. (A) BW gain, food intake, lean mass, and fat mass gain of aP2-ASKO (a) and Adn-ASKO (b) mice ($n = 8$) fed a standard chow diet. (B) Fat pad and liver weights of aP2-ASKO (a) and Adn-ASKO (b, right side) mice ($n = 8$). Data from male Adn-ASKO mice on a chow diet at 16 weeks of age (b, left side) and gonadal (Gon), inguinal (Ing), renal (Reno), and liver samples from these mice (b, middle) are also shown. (C) Hematoxylin-and-eosin staining of gonadal fat pads (left) and quantification of cell size (right, $n = 3$). Scale bar = 20 μm. (D) TAG contents (left), relative levels of DAG (middle), and FFA levels (right). The levels in Flox/Flox mice were defined as 100% (middle and right, $n = 4$). (E) Serum FFA levels in aP2-ASKO (a) and Adn-ASKO (b) mice ($n = 4$). (F, a) RT-qPCR for lipogenic gene expression in WAT ($n = 4$). (F, b) Immunoblotting of WAT lysates with antibodies to ACC, phosphorylated ACC (P-S79ACC), and AMPKα. GAPDH was used as an internal control. (F, c) Lipids generated were measured by counting [^{14}C]TAG after incubation of gonadal WAT fragments (with or without treatment with insulin at 1 μg/ml for 15 min) with D-[6-^{14}C]glucose for 2 h. Lipids were separated by TLC. Experiments were repeated twice, and representative data are shown. Data are expressed as means ± SEM. *, $P < 0.05$; **, $P < 0.01$; NS, no significant change.

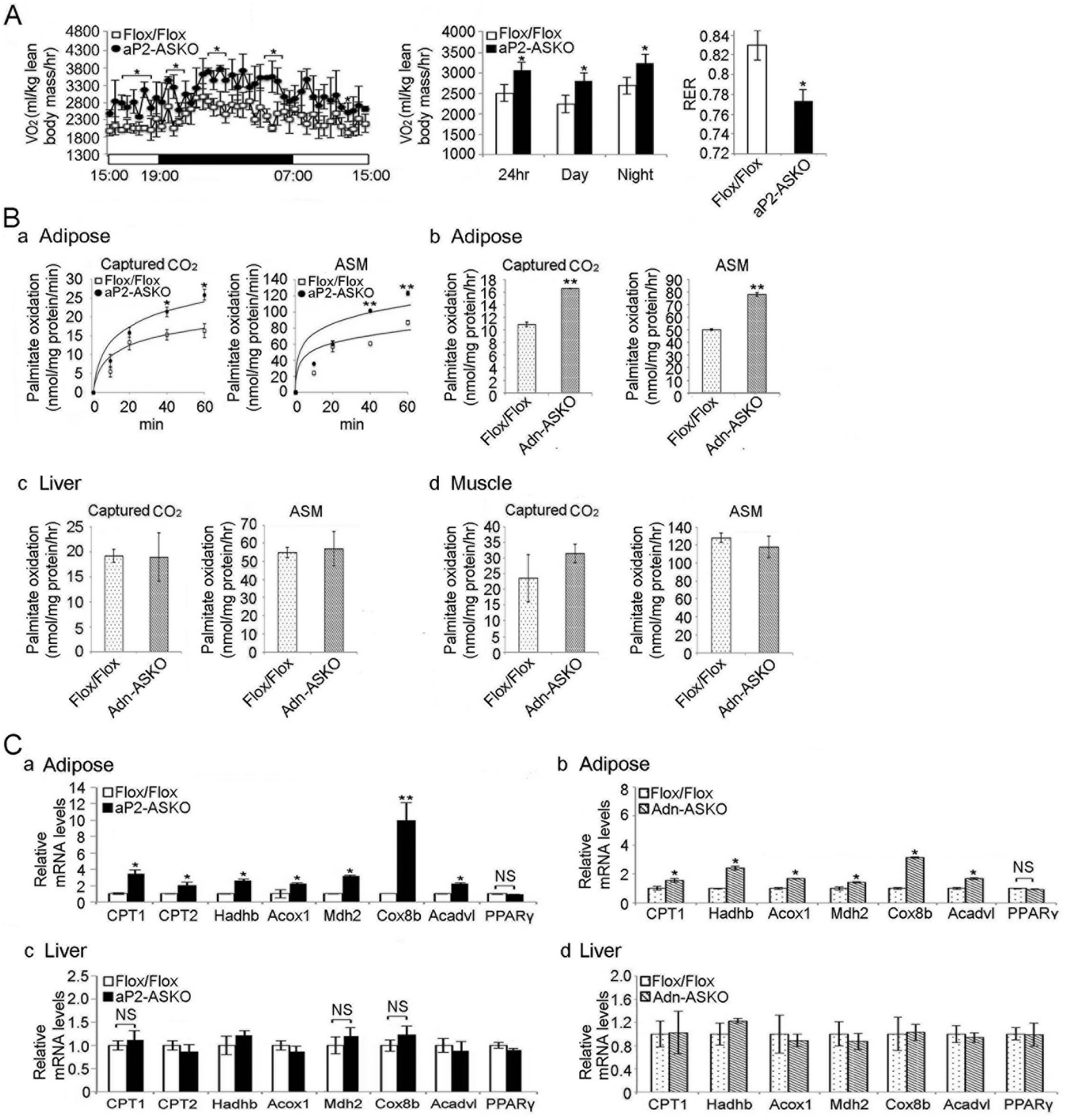

FIG 6 AMPKα1/α2 ablation promotes FA oxidation in adipose tissue. (A) O_2 consumption rate (VO_2) determined by indirect calorimetry in 16-week-old mice on a chow diet (left and middle; $n = 6$). The RER is shown on the right. (B) FA oxidation was measured by determining captured CO_2 and ASMs after the incubation of lysates with [^{14}C]palmitate for aP2-ASKO (a) and Adn-ASKO (b) mouse WAT, Adn-ASKO mouse liver (c), and Adn-ASKO mouse muscle (d). ($n = 4$). (C) RT-qPCR for FA oxidative genes in aP2-ASKO (a) and Adn-ASKO (b) mouse WAT and aP2-ASKO (c) and Adn-ASKO (d) mouse liver ($n = 4$). Data are expressed as means ± SEM. *, $P < 0.05$; **, $P < 0.01$; NS, no significant change.

adipose tissue of AMPK-ASKO mice, allowing HSL phosphorylation at S563 and S660 to increase its activity (Fig. 7E). The aberrantly high HSL activity in AMPK-ASKO mice was also evidenced by greater HSL binding to perilipin, accompanying markedly lower intracellular DAG levels, with an increase in total lipase activity. Therefore, for the first time, we demonstrate *in vivo* that HSL is under this interactive regulation of PKA and AMPK and that AMPK has an inhibitory effect on PKA-mediated phosphorylation/activation of HSL under stimulated conditions.

We previously reported that global AMPKα2 KO resulted in

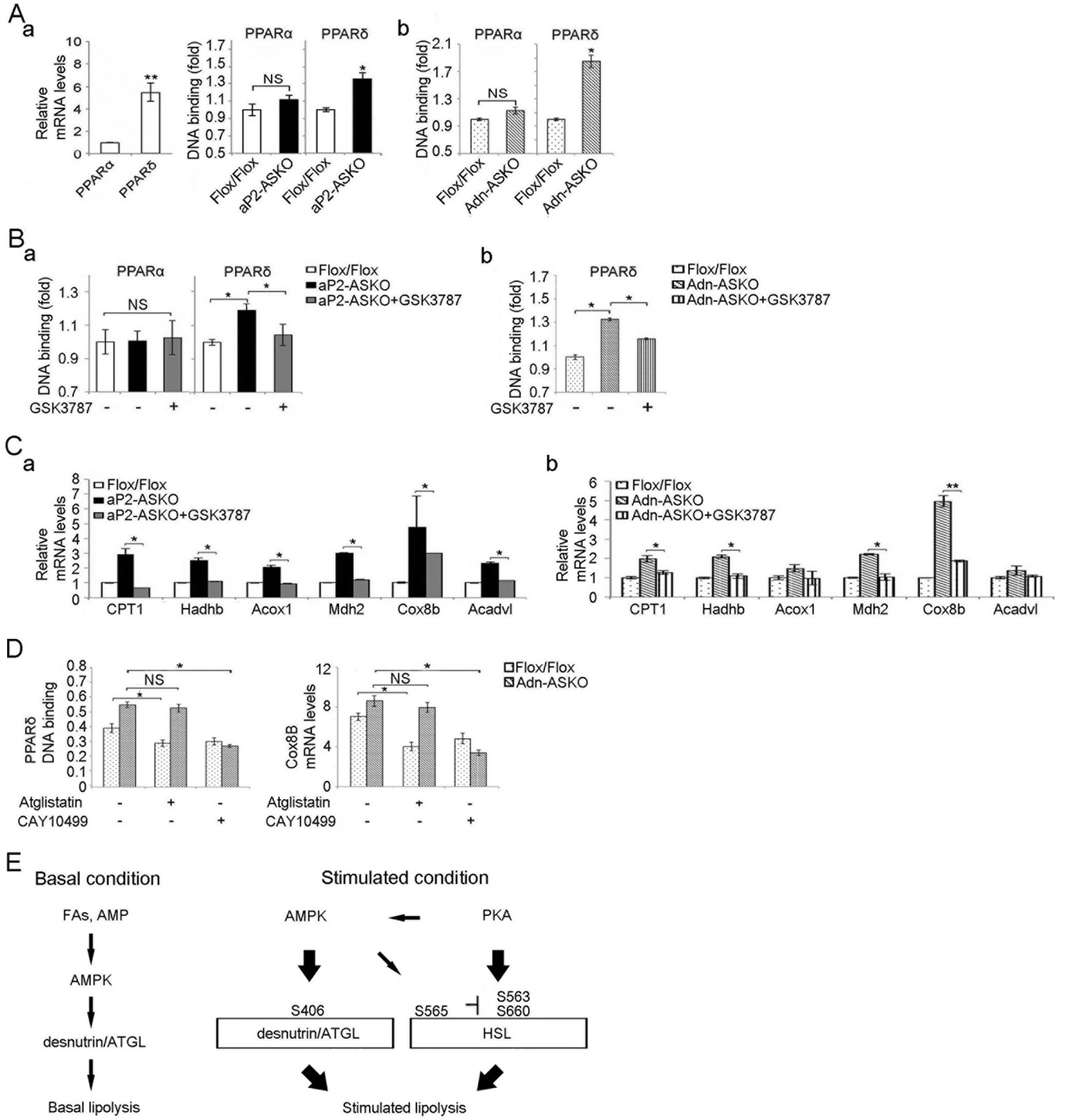

FIG 7 AMPKα1/α2 ablation promotes FA oxidation through PPARδ. (A) RT-qPCR for PPARα and PPARδ expression in WAT (a, left). PPARα and PPARδ binding activities in nuclear extracts from aP2-ASKO (a, right) and Adn-ASKO (b) mice are shown. (B) PPARα and PPARδ binding activities in WAT after GSK3787 injection for 3 days in aP2-ASKO (a) and Adn-ASKO (b) mice ($n = 5$). (C) Expression of FA oxidative genes in GSK3787-treated mice ($n = 5$) (a and b). (D) PPARδ binding activity (absorbance at 450 nm) and Cox8b ($2^{-\Delta\Delta CT}$) mRNA levels from Adn-ASKO mouse WAT explants upon treatment with 50 μM atglistatin ($n = 4$) or 10 μM CAY10499 ($n = 4$). Data are expressed as means ± SEM. *, $P < 0.05$; **$P < 0.01$; NS, no significant change. Experiments were repeated twice. (E) Function of AMPK in adipose lipolysis.

mice with an exacerbated adiposity phenotype (43). In this regard, AMPK activation increases glucose uptake and also induces FA oxidation to provide the energy needed in many tissues (4, 5). AMPK-induced FA oxidation may be through phosphorylation of ACC to inactivate its enzyme activity, resulting in a decrease in the concentration of malonyl-CoA and alleviating the inhibition of CPT1, allowing the entry of FA into mitochondria for oxidation. FA oxidation, as affected by lack of AMPK in a global fashion, may

have exacerbated adiposity from the HFD, because of less FA oxidation in various other tissues, not a cell-autonomous effect of AMPK deficiency in WAT. In contrast to mice with global AMPKα2 ablation, mice with adipose-tissue-specific KO of AMPKα1 and -α2 in the present study had a lean phenotype with increased lipolysis. FA oxidation and FA oxidative gene expression, as well as oxygen consumption, were higher in adipose tissue of AMPK-ASKO mice. A lower RER further indicates greater FA utilization in AMPK-ASKO mice. In this regard, FAs are known to be involved in cellular signaling pathways and regulation of gene transcription. FAs or their derivatives, as a ligand, can bind and activate the nuclear receptor family of transcription factors, PPARs. Desnutrin/ATGL-deficient mice with impaired lipolysis exhibited a severe defect in PPARα signaling in oxidative tissues such as BAT (15), liver (54), macrophages (55), and cardiac muscle (56). In addition, adipose-tissue-specific overexpression of PPARδ in mice has been shown to enhance the expression of genes for FA oxidation (57). Here, we show that because of ablation of AMPK in adipose tissue, FAs from increased lipolysis activated PPARδ in WAT and, as a consequence, FA oxidation was higher within WAT. In this regard, desnutrin/ATGL-derived FAs were previously shown to activate PPARδ for insulin secretion in islet β cells (58). It can be proposed that FA from lipolysis can activate all PPARs, but the abundance of a specific transcription factor in a tissue may be critical.

Here, we provide physiologically relevant *in vivo* evidence of opposing AMPK regulation of two regulatory enzymes in lipolysis, desnutrin/ATGL and HSL: activation of desnutrin/ATGL by S406 phosphorylation under basal conditions versus inhibition of HSL by S565 phosphorylation preventing PKA phosphorylation of S563 and S660 under stimulated conditions. Moreover, our present study of AMPK-ASKO mice reveals that, in contrast to other tissues, AMPK has a suppressive effect on FA oxidation and energy use within adipose tissue by lowering overall lipolysis. It also highlights the importance of FAs generated from lipolysis within adipocytes to activate PPARδ for induction of FA oxidative genes.

ACKNOWLEDGMENTS

We thank Sean J. Morrison for providing AMPKα1- and AMPKα2-floxed mice.

This work was supported by DK93928 to H.S.S.

S.-J.K., T.T., and M.A. generated the AMPK-ASKO mice. S.-J.K. and T.T. carried out the *in vivo* studies. H.S.S., S.-J.K., T.T., J.A.V., and Y.W. prepared the manuscript. H.S.S. designed the project, oversaw its performance, and provided data interpretation.

FUNDING INFORMATION

This work, including the efforts of Hei Sook Sul, was funded by HHS | National Institutes of Health (NIH) (DK93928).

REFERENCES

1. **Choi YH, Park S, Hockman S, Zmuda-Trzebiatowska E, Svennelid F, Haluzik M, Gavrilova O, Ahmad F, Pepin L, Napolitano M, Taira M, Sundler F, Stenson Holst L, Degerman E, Manganiello VC.** 2006. Alterations in the regulation of energy homeostasis in cyclic nucleotide phosphodiesterase 3B-null mice. J Clin Invest **116:**3240–3251. http://dx.doi.org/10.1172/JCI24867.
2. **Woods A, Cheung PC, Smith FC, Davison MD, Scott J, Beri RK, Carling D.** 1996. Characterization of AMP-activated protein kinase beta and gamma subunits. Assembly of the heterotrimeric complex in vitro. J Biol Chem **271:**10282–10290.
3. **Hawley SA, Davison M, Woods A, Davies SP, Beri RK, Carling D, Hardie DG.** 1996. Characterization of the AMP-activated protein kinase kinase from rat liver and identification of threonine 172 as the major site at which it phosphorylates AMP-activated protein kinase. J Biol Chem **271:**27879–27887. http://dx.doi.org/10.1074/jbc.271.44.27879.
4. **Carling D, Thornton C, Woods A, Sanders MJ.** 2012. AMP-activated protein kinase: new regulation, new roles? Biochem J **445:**11–27. http://dx.doi.org/10.1042/BJ20120546.
5. **Hardie DG, Ross FA, Hawley SA.** 2012. AMPK: a nutrient and energy sensor that maintains energy homeostasis. Nat Rev Mol Cell Biol **13:**251–262. http://dx.doi.org/10.1038/nrm3311.
6. **Zhang BB, Zhou G, Li C.** 2009. AMPK: an emerging drug target for diabetes and the metabolic syndrome. Cell Metab **9:**407–416. http://dx.doi.org/10.1016/j.cmet.2009.03.012.
7. **Li Y, Xu S, Mihaylova MM, Zheng B, Hou X, Jiang B, Park O, Luo Z, Lefai E, Shyy JY, Gao B, Wierzbicki M, Verbeuren TJ, Shaw RJ, Cohen RA, Zang M.** 2011. AMPK phosphorylates and inhibits SREBP activity to attenuate hepatic steatosis and atherosclerosis in diet-induced insulin-resistant mice. Cell Metab **13:**376–388. http://dx.doi.org/10.1016/j.cmet.2011.03.009.
8. **Villena JA, Roy S, Sarkadi-Nagy E, Kim KH, Sul HS.** 2004. Desnutrin, an adipocyte gene encoding a novel patatin domain-containing protein, is induced by fasting and glucocorticoids: ectopic expression of desnutrin increases triglyceride hydrolysis. J Biol Chem **279:**47066–47075. http://dx.doi.org/10.1074/jbc.M403855200.
9. **Jenkins CM, Mancuso DJ, Yan W, Sims HF, Gibson B, Gross RW.** 2004. Identification, cloning, expression, and purification of three novel human calcium-independent phospholipase A2 family members possessing triacylglycerol lipase and acylglycerol transacylase activities. J Biol Chem **279:**48968–48975. http://dx.doi.org/10.1074/jbc.M407841200.
10. **Eichmann TO, Kumari M, Haas JT, Farese RV, Jr, Zimmermann R, Lass A, Zechner R.** 2012. Studies on the substrate and stereo/regioselectivity of adipose triglyceride lipase, hormone-sensitive lipase, and diacylglycerol-O-acyltransferases. J Biol Chem **287:**41446–41457. http://dx.doi.org/10.1074/jbc.M112.400416.
11. **Zimmermann R, Strauss JG, Haemmerle G, Schoiswohl G, Birner-Gruenberger R, Riederer M, Lass A, Neuberger G, Eisenhaber F, Hermetter A, Zechner R.** 2004. Fat mobilization in adipose tissue is promoted by adipose triglyceride lipase. Science **306:**1383–1386. http://dx.doi.org/10.1126/science.1100747.
12. **Frühbeck G, Mendez-Gimenez L, Fernandez-Formoso JA, Fernandez S, Rodriguez A.** 2014. Regulation of adipocyte lipolysis. Nutr Res Rev **27:**63–93. http://dx.doi.org/10.1017/S095442241400002X.
13. **Ahmadian M, Duncan RE, Varady KA, Frasson D, Hellerstein MK, Birkenfeld AL, Samuel VT, Shulman GI, Wang Y, Kang C, Sul HS.** 2009. Adipose overexpression of desnutrin promotes fatty acid use and attenuates diet-induced obesity. Diabetes **58:**855–866. http://dx.doi.org/10.2337/db08-1644.
14. **Haemmerle G, Lass A, Zimmermann R, Gorkiewicz G, Meyer C, Rozman J, Heldmaier G, Maier R, Theussl C, Eder S, Kratky D, Wagner EF, Klingenspor M, Hoefler G, Zechner R.** 2006. Defective lipolysis and altered energy metabolism in mice lacking adipose triglyceride lipase. Science **312:**734–737. http://dx.doi.org/10.1126/science.1123965.
15. **Ahmadian M, Abbott MJ, Tang T, Hudak CS, Kim Y, Bruss M, Hellerstein MK, Lee HY, Samuel VT, Shulman GI, Wang Y, Duncan RE, Kang C, Sul HS.** 2011. Desnutrin/ATGL is regulated by AMPK and is required for a brown adipose phenotype. Cell Metab **13:**739–748. http://dx.doi.org/10.1016/j.cmet.2011.05.002.
16. **Yeaman SJ.** 1990. Hormone-sensitive lipase—a multipurpose enzyme in lipid metabolism. Biochim Biophys Acta **1052:**128–132. http://dx.doi.org/10.1016/0167-4889(90)90067-N.
17. **Lass A, Zimmermann R, Oberer M, Zechner R.** 2011. Lipolysis—a highly regulated multi-enzyme complex mediates the catabolism of cellular fat stores. Prog Lipid Res **50:**14–27. http://dx.doi.org/10.1016/j.plipres.2010.10.004.
18. **Haemmerle G, Zimmermann R, Strauss JG, Kratky D, Riederer M, Knipping G, Zechner R.** 2002. Hormone-sensitive lipase deficiency in mice changes the plasma lipid profile by affecting the tissue-specific expression pattern of lipoprotein lipase in adipose tissue and muscle. J Biol Chem **277:**12946–12952. http://dx.doi.org/10.1074/jbc.M108640200.
19. **Osuga J, Ishibashi S, Oka T, Yagyu H, Tozawa R, Fujimoto A, Shionoiri F, Yahagi N, Kraemer FB, Tsutsumi O, Yamada N.** 2000. Targeted disruption of hormone-sensitive lipase results in male sterility and adi-

pocyte hypertrophy, but not in obesity. Proc Natl Acad Sci U S A **97:**787–792. http://dx.doi.org/10.1073/pnas.97.2.787.
20. **Frayn KN, Karpe F, Fielding BA, Macdonald IA, Coppack SW.** 2003. Integrative physiology of human adipose tissue. Int J Obes Relat Metab Disord **27:**875–888. http://dx.doi.org/10.1038/sj.ijo.0802326.
21. **Anthonsen MW, Ronnstrand L, Wernstedt C, Degerman E, Holm C.** 1998. Identification of novel phosphorylation sites in hormone-sensitive lipase that are phosphorylated in response to isoproterenol and govern activation properties in vitro. J Biol Chem **273:**215–221. http://dx.doi.org/10.1074/jbc.273.1.215.
22. **Anthony NM, Gaidhu MP, Ceddia RB.** 2009. Regulation of visceral and subcutaneous adipocyte lipolysis by acute AICAR-induced AMPK activation. Obesity (Silver Spring) **17:**1312–1317. http://dx.doi.org/10.1038/oby.2008.645.
23. **Yeaman SJ.** 2004. Hormone-sensitive lipase—new roles for an old enzyme. Biochem J **379:**11–22. http://dx.doi.org/10.1042/bj20031811.
24. **Sullivan JE, Brocklehurst KJ, Marley AE, Carey F, Carling D, Beri RK.** 1994. Inhibition of lipolysis and lipogenesis in isolated rat adipocytes with AICAR, a cell-permeable activator of AMP-activated protein kinase. FEBS Lett **353:**33–36. http://dx.doi.org/10.1016/0014-5793(94)01006-4.
25. **Corton JM, Gillespie JG, Hawley SA, Hardie DG.** 1995. 5-Aminoimidazole-4-carboxamide ribonucleoside. A specific method for activating AMP-activated protein kinase in intact cells? Eur J Biochem **229:**558–565.
26. **Watt MJ, Holmes AG, Pinnamaneni SK, Garnham AP, Steinberg GR, Kemp BE, Febbraio MA.** 2006. Regulation of HSL serine phosphorylation in skeletal muscle and adipose tissue. Am J Physiol Endocrinol Metab **290:**E500–E508.
27. **Hutchinson DS, Chernogubova E, Dallner OS, Cannon B, Bengtsson T.** 2005. Beta-adrenoceptors, but not alpha-adrenoceptors, stimulate AMP-activated protein kinase in brown adipocytes independently of uncoupling protein-1. Diabetologia **48:**2386–2395. http://dx.doi.org/10.1007/s00125-005-1936-7.
28. **Omar B, Zmuda-Trzebiatowska E, Manganiello V, Goransson O, Degerman E.** 2009. Regulation of AMP-activated protein kinase by cAMP in adipocytes: roles for phosphodiesterases, protein kinase B, protein kinase A, Epac and lipolysis. Cell Signal **21:**760–766. http://dx.doi.org/10.1016/j.cellsig.2009.01.015.
29. **Djouder N, Tuerk RD, Suter M, Salvioni P, Thali RF, Scholz R, Vaahtomeri K, Auchli Y, Rechsteiner H, Brunisholz RA, Viollet B, Makela TP, Wallimann T, Neumann D, Krek W.** 2010. PKA phosphorylates and inactivates AMPKalpha to promote efficient lipolysis. EMBO J **29:**469–481. http://dx.doi.org/10.1038/emboj.2009.339.
30. **Nakada D, Saunders TL, Morrison SJ.** 2010. Lkb1 regulates cell cycle and energy metabolism in haematopoietic stem cells. Nature **468:**653–658. http://dx.doi.org/10.1038/nature09571.
31. **He W, Barak Y, Hevener A, Olson P, Liao D, Le J, Nelson M, Ong E, Olefsky JM, Evans RM.** 2003. Adipose-tissue-specific peroxisome proliferator-activated receptor gamma knockout causes insulin resistance in fat and liver but not in muscle. Proc Natl Acad Sci U S A **100:**15712–15717. http://dx.doi.org/10.1073/pnas.2536828100.
32. **Schweiger M, Eichmann TO, Taschler U, Zimmermann R, Zechner R, Lass A.** 2014. Measurement of lipolysis. Methods Enzymol **538:**171–193. http://dx.doi.org/10.1016/B978-0-12-800280-3.00010-4.
33. **Folch J, Lees M, Sloane Stanley GH.** 1957. A simple method for the isolation and purification of total lipides from animal tissues. J Biol Chem **226:**497–509.
34. **Jeffery E, Berry R, Church CD, Yu S, Shook BA, Horsley V, Rosen ED, Rodeheffer MS.** 2014. Characterization of Cre recombinase models for the study of adipose tissue. Adipocyte **3:**206–211. http://dx.doi.org/10.4161/adip.29674.
35. **Garton AJ, Campbell DG, Carling D, Hardie DG, Colbran RJ, Yeaman SJ.** 1989. Phosphorylation of bovine hormone-sensitive lipase by the AMP-activated protein kinase. A possible antilipolytic mechanism. Eur J Biochem **179:**249–254.
36. **Yin W, Mu J, Birnbaum MJ.** 2003. Role of AMP-activated protein kinase in cyclic AMP-dependent lipolysis in 3T3-L1 adipocytes. J Biol Chem **278:**43074–43080. http://dx.doi.org/10.1074/jbc.M308484200.
37. **Clifford GM, Londos C, Kraemer FB, Vernon RG, Yeaman SJ.** 2000. Translocation of hormone-sensitive lipase and perilipin upon lipolytic stimulation of rat adipocytes. J Biol Chem **275:**5011–5015. http://dx.doi.org/10.1074/jbc.275.7.5011.
38. **Wang H, Hu L, Dalen K, Dorward H, Marcinkiewicz A, Russell D, Gong D, Londos C, Yamaguchi T, Holm C, Rizzo MA, Brasaemle D, Sztalryd C.** 2009. Activation of hormone-sensitive lipase requires two steps, protein phosphorylation and binding to the PAT-1 domain of lipid droplet coat proteins. J Biol Chem **284:**32116–32125. http://dx.doi.org/10.1074/jbc.M109.006726.
39. **Foretz M, Pacot C, Dugail I, Lemarchand P, Guichard C, Le Liepvre X, Berthelier-Lubrano C, Spiegelman B, Kim JB, Ferre P, Foufelle F.** 1999. ADD1/SREBP-1c is required in the activation of hepatic lipogenic gene expression by glucose. Mol Cell Biol **19:**3760–3768. http://dx.doi.org/10.1128/MCB.19.5.3760.
40. **Zhou G, Myers R, Li Y, Chen Y, Shen X, Fenyk-Melody J, Wu M, Ventre J, Doebber T, Fujii N, Musi N, Hirshman MF, Goodyear LJ, Moller DE.** 2001. Role of AMP-activated protein kinase in mechanism of metformin action. J Clin Invest **108:**1167–1174. http://dx.doi.org/10.1172/JCI13505.
41. **Orci L, Cook WS, Ravazzola M, Wang MY, Park BH, Montesano R, Unger RH.** 2004. Rapid transformation of white adipocytes into fat-oxidizing machines. Proc Natl Acad Sci U S A **101:**2058–2063. http://dx.doi.org/10.1073/pnas.0308258100.
42. **Madrazo JA, Kelly DP.** 2008. The PPAR trio: regulators of myocardial energy metabolism in health and disease. J Mol Cell Cardiol **44:**968–975. http://dx.doi.org/10.1016/j.yjmcc.2008.03.021.
43. **Villena JA, Viollet B, Andreelli F, Kahn A, Vaulont S, Sul HS.** 2004. Induced adiposity and adipocyte hypertrophy in mice lacking the AMP-activated protein kinase-alpha2 subunit. Diabetes **53:**2242–2249. http://dx.doi.org/10.2337/diabetes.53.9.2242.
44. **Gaidhu MP, Frontini A, Hung S, Pistor K, Cinti S, Ceddia RB.** 2011. Chronic AMP-kinase activation with AICAR reduces adiposity by remodeling adipocyte metabolism and increasing leptin sensitivity. J Lipid Res **52:**1702–1711. http://dx.doi.org/10.1194/jlr.M015354.
45. **Bartz R, Zehmer JK, Zhu M, Chen Y, Serrero G, Zhao Y, Liu P.** 2007. Dynamic activity of lipid droplets: protein phosphorylation and GTP-mediated protein translocation. J Proteome Res **6:**3256–3265. http://dx.doi.org/10.1021/pr070158j.
46. **Pagnon J, Matzaris M, Stark R, Meex RC, Macaulay SL, Brown W, O'Brien PE, Tiganis T, Watt MJ.** 2012. Identification and functional characterization of protein kinase A phosphorylation sites in the major lipolytic protein, adipose triglyceride lipase. Endocrinology **153:**4278–4289. http://dx.doi.org/10.1210/en.2012-1127.
47. **Narbonne P, Roy R.** 2009. Caenorhabditis elegans dauers need LKB1/AMPK to ration lipid reserves and ensure long-term survival. Nature **457:**210–214. http://dx.doi.org/10.1038/nature07536.
48. **Gaidhu MP, Fediuc S, Anthony NM, So M, Mirpourian M, Perry RL, Ceddia RB.** 2009. Prolonged AICAR-induced AMP-kinase activation promotes energy dissipation in white adipocytes: novel mechanisms integrating HSL and ATGL. J Lipid Res **50:**704–715. http://dx.doi.org/10.1194/jlr.M800480-JLR200.
49. **Lass A, Zimmermann R, Haemmerle G, Riederer M, Schoiswohl G, Schweiger M, Kienesberger P, Strauss JG, Gorkiewicz G, Zechner R.** 2006. Adipose triglyceride lipase-mediated lipolysis of cellular fat stores is activated by CGI-58 and defective in Chanarin-Dorfman syndrome. Cell Metab **3:**309–319. http://dx.doi.org/10.1016/j.cmet.2006.03.005.
50. **Miyoshi H, Perfield JW, II, Obin MS, Greenberg AS.** 2008. Adipose triglyceride lipase regulates basal lipolysis and lipid droplet size in adipocytes. J Cell Biochem **105:**1430–1436. http://dx.doi.org/10.1002/jcb.21964.
51. **Liu Q, Gauthier MS, Sun L, Ruderman N, Lodish H.** 2010. Activation of AMP-activated protein kinase signaling pathway by adiponectin and insulin in mouse adipocytes: requirement of acyl-CoA synthetases FATP1 and Acsl1 and association with an elevation in AMP/ATP ratio. FASEB J **24:**4229–4239. http://dx.doi.org/10.1096/fj.10-159723.
52. **Londos C, Brasaemle DL, Schultz CJ, Adler-Wailes DC, Levin DM, Kimmel AR, Rondinone CM.** 1999. On the control of lipolysis in adipocytes. Ann N Y Acad Sci **892:**155–168. http://dx.doi.org/10.1111/j.1749-6632.1999.tb07794.x.
53. **Garton AJ, Yeaman SJ.** 1990. Identification and role of the basal phosphorylation site on hormone-sensitive lipase. Eur J Biochem **191:**245–250. http://dx.doi.org/10.1111/j.1432-1033.1990.tb19116.x.
54. **Ong KT, Mashek MT, Bu SY, Greenberg AS, Mashek DG.** 2011. Adipose triglyceride lipase is a major hepatic lipase that regulates triacylglycerol turnover and fatty acid signaling and partitioning. Hepatology **53:**116–126. http://dx.doi.org/10.1002/hep.24006.
55. **Chandak PG, Radovic B, Aflaki E, Kolb D, Buchebner M, Frohlich E, Magnes C, Sinner F, Haemmerle G, Zechner R, Tabas I, Levak-Frank S,**

Kratky D. 2010. Efficient phagocytosis requires triacylglycerol hydrolysis by adipose triglyceride lipase. J Biol Chem **285:**20192–20201. http://dx.doi.org/10.1074/jbc.M110.107854.

56. **Haemmerle G, Moustafa T, Woelkart G, Buttner S, Schmidt A, van de Weijer T, Hesselink M, Jaeger D, Kienesberger PC, Zierler K, Schreiber R, Eichmann T, Kolb D, Kotzbeck P, Schweiger M, Kumari M, Eder S, Schoiswohl G, Wongsiriroj N, Pollak NM, Radner FP, Preiss-Landl K, Kolbe T, Rulicke T, Pieske B, Trauner M, Lass A, Zimmermann R, Hoefler G, Cinti S, Kershaw EE, Schrauwen P, Madeo F, Mayer B, Zechner R.** 2011. ATGL-mediated fat catabolism regulates cardiac mitochondrial function via PPAR-alpha and PGC-1. Nat Med **17:**1076–1085. http://dx.doi.org/10.1038/nm.2439.
57. **Wang YX, Lee CH, Tiep S, Yu RT, Ham J, Kang H, Evans RM.** 2003. Peroxisome-proliferator-activated receptor delta activates fat metabolism to prevent obesity. Cell **113:**159–170. http://dx.doi.org/10.1016/S0092-8674(03)00269-1.
58. **Tang T, Abbott MJ, Ahmadian M, Lopes AB, Wang Y, Sul HS.** 2013. Desnutrin/ATGL activates PPARdelta to promote mitochondrial function for insulin secretion in islet beta cells. Cell Metab **18:**883–895. http://dx.doi.org/10.1016/j.cmet.2013.10.012.